VYSOKÉ UČENÍ TECHNICKÉ V BRNĚ

BRNO UNIVERSITY OF TECHNOLOGY

FAKULTA STROJNÍHO INŽENÝRSTVÍ

FACULTY OF MECHANICAL ENGINEERING

ÚSTAV FYZIKÁLNÍHO INŽENÝRSTVÍ

INSTITUTE OF PHYSICAL ENGINEERING

STUDIUM ELEKTRONICKÉ ODEZVY DVOUHRADLOVÉHO GRAFENOVÉHO SELEKTIVNÍHO BIOSENZORU

ELECTRONIC RESPONSE STUDY OF A DUAL-GATE GRAPHENE SELECTIVE BIOSENSOR

BAKALÁŘSKÁ PRÁCE

BACHELOR'S THESIS

AUTOR PRÁCE — **ONDŘEJ BRDEČKO**

AUTHOR

VEDOUCÍ PRÁCE — **doc. Ing. MIROSLAV BARTOŠÍK, Ph.D.**

SUPERVISOR

BRNO 2023

BRNO UNIVERSITY OF TECHNOLOGY
FACULTY OF MECHANICAL ENGINEERING

Assignment Bachelor's Thesis

Institut:	Institute of Physical Engineering
Student:	**Ondřej Brdečko**
Degree programm:	Physical Engineering and Nanotechnology
Branch:	no specialisation
Supervisor:	**doc. Ing. Miroslav Bartošík, Ph.D.**
Academic year:	2022/23

As provided for by the Act No. 111/98 Coll. on higher education institutions and the BUT Study and Examination Regulations, the director of the Institute hereby assigns the following topic of Bachelor's Thesis:

Electronic response study of a dual–gate graphene selective biosensor

Brief Description:

Low electronic noise, high surface sensitivity to adsorbents, biocompatibility and the possibility of functionalization predetermine graphene for utilizing in biosensors. As part of this work, a graphene two–point selective glucose sensor will be fabricated in a field–effect transistor (FET) architecture with a lower solid–state gate and an upper gate connected through the detected solution. The possibility of increasing the resistance response of the sensor to glucose through the setting of both gates will then be studied on the device prepared in this way. The effect of the electric field of both gates on the stability of functionalized graphene will also be verified.

Bachelor's Thesis goals:

1. Do research on the mentioned issue.
2. Perform chemical functionalization of graphene Hall bars for glucose biosensor.
3. Study the transport response of the biosensor to a solution of a suitable concentration of glucose as a function of voltage applied on:
a. Upper gate.
b. Lower gate.
c. Both gates.
4. Before and after the measurement, verify the stability of the functionalization using Raman spectroscopy and possibly AFM.

Recommended bibliography:

SCHEDIN, F., A. K. GEIM, S. V. MOROZOV, E. W. HILL, P. BLAKE, M. I. KATSNELSON a K. S. NOVOSELOV. Detection of individual gas molecules adsorbed on graphene. Nature Materials. 2007, 6(9), 652-655. DOI: 10.1038/nmat1967.

SHAO, Y., J. WANG, H. WU, J. LIU, I. A. AKSAY, Y. LIN. Graphene Based Electrochemical Sensors and Biosensors: A Review. Electroanalysis. 2010, 22(10), 1027-1036. DOI: 10.1002/elan.200900571.

NAG, A., A. MITRA, S. C. MUKHOPADHYAY. Graphene and its sensor-based applications: A review. Sensors and Actuators A: Physical. 2018, 270, 177-194. DOI: 10.1016/j.sna.2017.12.028.

KWAK, Y. H., D. S. CHOI, Y. N. KIM, H. KIM, D. H. YOON, S. S. AHN, J. W. YANG, W. S. YANG, S. SEO. Flexible glucose sensor using CVD-grown graphene-based field effect transistor. Biosensors and Bioelectronics. 2012, 37(1), 82-87. DOI: 10.1016/j.bios.2012.04.042

SHAN, C., H. YANG, J. SONG, D. HAN, A. IVASKA, L. NIU. Direct Electrochemistry of Glucose Oxidase and Biosensing for Glucose Based on Graphene. Analytical Chemistry. 2009, 81(6), 2378-2382. DOI: 10.1021/ac802193c

ZHU, Zanzan. An Overview of Carbon Nanotubes and Graphene for Biosensing Applications. NanoMicro Letters. 2017, 9(3), 1-24. DOI: 10.1007/s40820-017-0128-6.

Deadline for submission Bachelor's Thesis is given by the Schedule of the Academic year 2022/23

In Brno,

L. S.

prof. RNDr. Tomáš Šikola, CSc. Director of the Institute	doc. Ing. Jiří Hlinka, Ph.D. FME dean

Abstrakt

Detekce glukózy je důležitá zejména kvůli diabetes mellitus, nemoci, která způsobuje nestabilní hladinu cukru v krvi. Kvůli této nemoci je potřeba spolehlivý senzor glukózy pro aplikaci v medicíně. V této práci je popsán dvouhradlový biosenzor na bázi grafenového polem řízeného tranzistoru a je zkoumána jeho odezva na roztoky glukózy o různých koncentracích. Odezva senzoru je zkoumána pro zapojení horního i spodního hradla.

Summary

Glucose sensing is important mainly because of the diabetes mellitus, a disease that causes unstable blood sugar level. Cause of this disease, reliable glucose sensor is needed for medical applications. In this thesis, a dual gated graphene field effect transistor biosensor for glucose sensing is described and its response on glucose solutions of different concentrations is tested. The sensor is tested for top gate configuration and bottom gate configuration.

Klíčová slova

Detekce glukózy, grafénový polem řízený tranzistor, dvojné hradlo

Keywords

Glucose sensing, graphene FET, double-gate

BRDEČKO, O. *Studium elektronické odezvy dvouhradlového grafenového selektivního biosenzoru*. Brno: Vysoké učení technické v Brně, Fakulta strojního inženýrství, 2023. 31 s. Vedoucí doc. Ing. Miroslav Bartošík, Ph.D.

I declare that I have written the Bachelor's Thesis titled *Electronic response study of a dual-gate graphene selective biosensor* independently, under the guidance of the advisor doc. Ing. Miroslav Bartošík, Ph.D. and using exclusively the technical references and other sources of information cited in the thesis and listed in the comprehensive bibliography at the end of the thesis.

Ondřej Brdečko

I would like to acknowledge my supervisor doc. Ing. Miroslav Barošík, Ph.D. for his patient guidance and helpful communication and to bc. Michaela Malatinová for explanation of the measuring procedure. Also to bc. Linda Supalová and Ing. Jakub Piastek for prepearation of the samples and for numerous advises.

Ondřej Brdečko

Contents

1. Introduction

Since 2004 when Geim and Novoselov isolated and investigated graphene as a carbon mono-layer, it has been of great interest in the electronic sensing processes (among other disciplines). Mainly thanks to its unique properties like its high tensile strength, high mobility of charge carriers and the linear dependence between the amount of charge carriers and applied gate voltage that in graphene is symmetrical around the Dirac point.

Graphene based sensors are capable of selective as well as non-selective sensing. Selective sensing requires a functionalization of graphene before measuring which is more demanding, but in most cases it can yield more precise results, making it an inevitable approach for certain applications.

This thesis is dedicated to the graphene based field effect transistor biosensor for measuring glucose concentration. The respective measuring process is performed via selective approach using glucose oxidase enzyme to bind glucose molecules.

There are several reasons for monitoring glucose concentration. Probably the most important reason is to determine glucose level in human blood especially for people who are diagnosed with a disease called diabetes mellitus. This disease causes that the blood sugar level is not regulated correctly. But glucose sensing is also important in food analysis.

One of the aims of this thesis and the belonging research is to prepare a dual gated sensor - a sensor, that can be loaded by top and bottom gate voltage at the same time. The already existing versions of this kind of sensor has already been tested for top gating as well as bottom gating, but it is involving both gates at the same time that this research aims to document.

The documentation of the sensor response for each gate allows us to compare them and determine which of them is more suitable for particular applications.

2. Biosensors

A biosensor is a device, that serves for monitoring a biochemical system. Usually it consists of a biological sensing element (e.g. enzyme, organelle, cell, ...) and a transducer, which converts the information about the state of the observed system from a biochemical signal to usually a digital electronic signal (Fig. 1). [1]

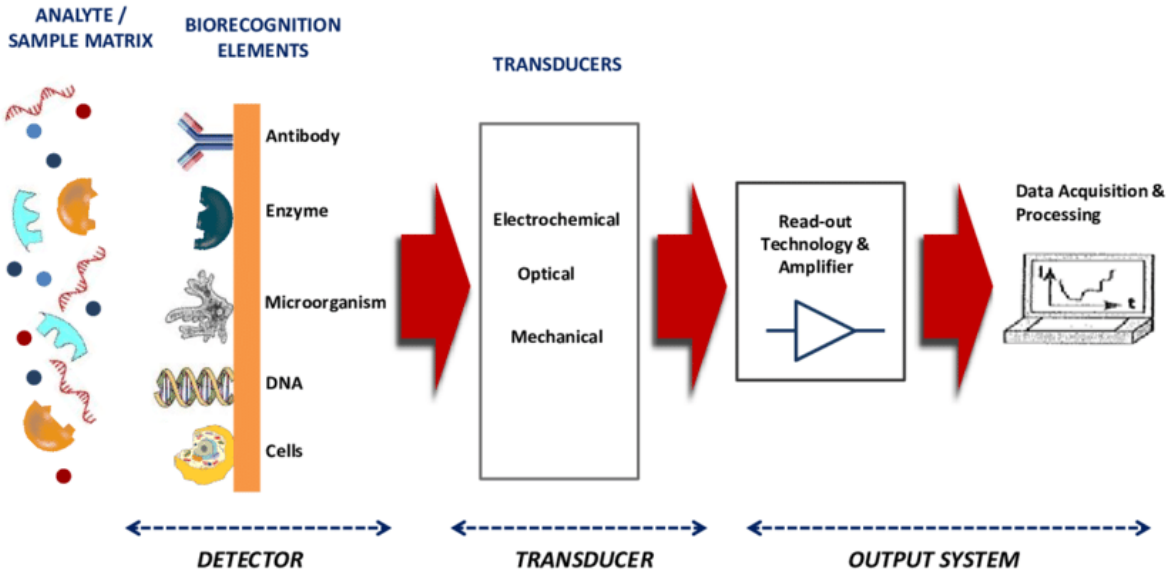

Fig. 1: Biosensor mechanism scheme. The analyte reacts with the bio-recognition element which produces some kind of electrical, mechanical or optical signal that is then transferred to an electronic device and processed. Adapted from [2].

There are many classifications of biosensors, but we can broadly differentiate 3 types, electrochemical, optical and piezoelectric (mass) sensors. [3]

The sensing of electrochemical sensors is based on a conversion of a biochemical process to an electrical signal. [6] "The typical transducer for an electrochemical biosensor is an electrode that translates the flow of ions generated by binding reactions between the analyte and the bio-recognition element into an electrical current or voltage." [4]

Piezoelectric sensors generally consist of a piezoelectric transducer element that vibrates with a characteristic frequency. The bio-recognition element is fastened to the piezoelectric part. The presence of the analyte changes the vibration frequency of the piezoelectric part. [5]

Optical biosensors

The essence of optical biosensors is in the interaction of the optical field with the bio-recognition element. [6]

This work is dedicated to a biosensor that belongs to the first mentioned type - electrochemical biosensors. It is a sensor that is used to detect glucose concentration in a solution. The bio-recognition element in the sensor is glucose oxidase.

3. Glucose detection - chemicals

The sensing mechanism used for glucose detection described in this thesis and used during the experiment requires several chemicals. In this chapter the chemicals are described.

β-D-glucose (Fig. 2) is a simple sugar that belongs to the group of hexoses. It has the ability to make a cyclic form called furanose (glucofuranose). Glucose is a product of photosynthesis in plant cells and it is the main source of energy in the human body. It can be ingested in food, upon which it is partially sent to the blood and mainly stored in liver in form of glycogen. There are 2 enzymes which regulate the blood sugar level. Insuline, which lowers the blood sugar level and glucagon, which increases it. D-glucose has a useful property of being an optical isomer, which means that its solution can change the plane of polarization of light that goes through it. [7][8]

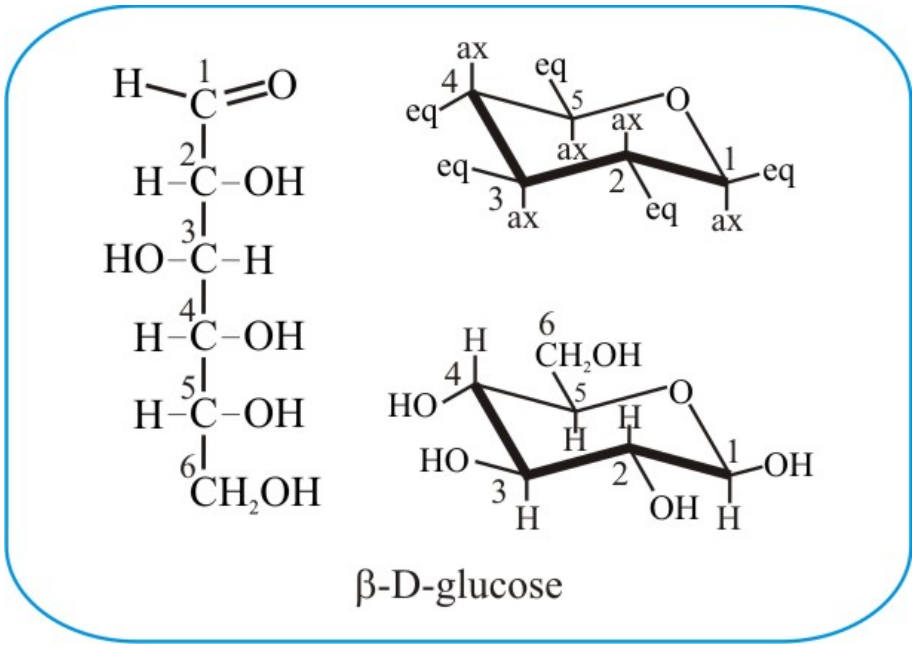

Fig. 2: β-D-glucose in a linear and cyclic form, adapted from [9]

Glucose oxidase is a dimeric catalytic enzyme, that catalyzes the conversion of β-D-glucose to D-glucono-1,5-lactone (Fig. 3). Glucose oxidase is useful for glucose detection because "it is active on a wide range of physiologically relevant glucose concentrations."[10] The chemical equation below shows the reaction of glucose-oxidase with the glucose. The

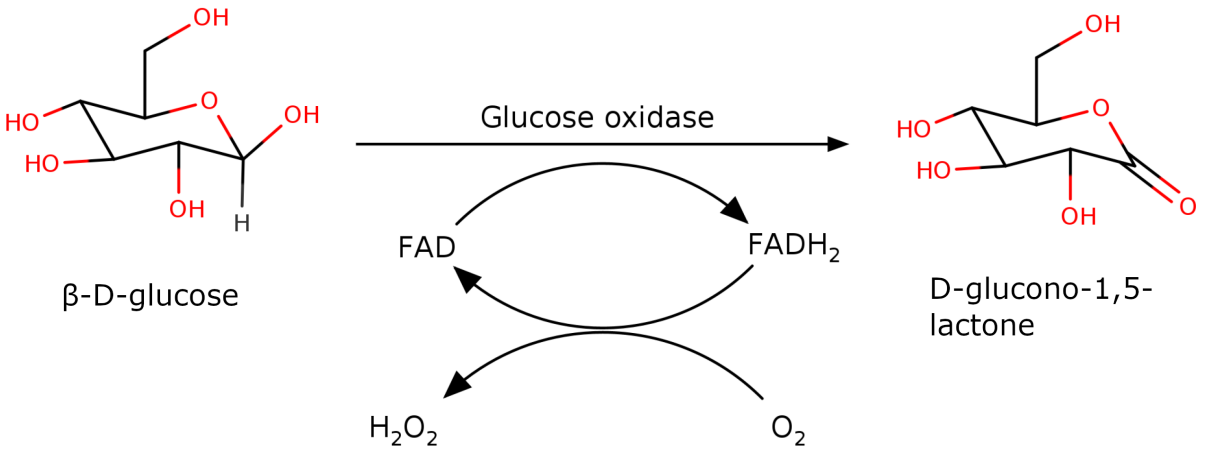

Fig. 3: Glucose oxidase reaction scheme (adapted from [11] and edited). Glucose oxidase transform β-D-glucose to D-glucono-1,5-lactone. During this process flavinadenindinucleotide (FAD) in the human body is reduced to $FADH_2$ by receiving two electrons and two protons. The backward oxidation is accompanied by a reduction of oxygen to hydrogen-peroxid.

other important advantage of glucose oxidase is its specific reactivity. It reacts with glucose but it doesn't react with other simple sugars, so it is used for specific detection.

NN-dimethyl formamide (DMF) is a solvent for chemical reactions. It is used for isolating chlorophyll in plants. It also plays a significant role as a solvent, catalyst, agent or reducing agent in many reactions. It is a precursor for several types of reactions as formylation, amination, aminocarboxylation, etc. During the sensor functionalization process it serves as a solvent for 1-Pyrenebutiric acid N-hydroxysuccinimide ester.[12]

1-Pyrenebutiric acid N-hydroxysuccinimide ester (PSE) is an aromatic chemical soluble in chloroform, N,N dimethyl formamide, dimethyl sulfoxide, and methanol. It is used in hematology, histology and diagnostic assay manufacturing. It can be stored at room temperature. In the sensing procedure it serves as a linker molecule for Glucoseoxidase. [27]

Phosphate buffer saline (PBS) is a powder soluble in water that in solution serves for washing processes in imunofluorescence procedures, as a suspension for bacterial cells or in imunostaining procedures. In the 0.01 M solution, it contains KCl 0.0027 M and NaCl 0.138 M. At room temperature its pH is about 7.4. During the functionalization

and measuring we used it in solution diluted in DI water in concentration 0.01 M as a solvent for glucose concentrations, and in 0.1 M concentrtion for rinsing of the graphene after glucose oxidase binding process.

4. Graphene

Graphene is a single-layer carbon material with a honeycomb lattice. Carbon lies in the 4.A group in the periodic system of elements, so it has 4 valence electrons. In the ground state there are two electrons in s orbital and each of the two remaining are separately in p orbitals. When sp^2 hybridization takes place, three of the valence electrons get in three sp^2 hybridized orbitals and the third electron occupies p orbital. The fourth electron is responsible for conducting or bending of molecules on the graphene surface. Thanks to this hybridization in graphene, each carbon atom is covalently bonded to the three closest neighbouring atoms. Due to the symmetry the binding angle is 120° which leads to the formation of the honeycomb lattice. The bond length is 1.42 Å.[14]

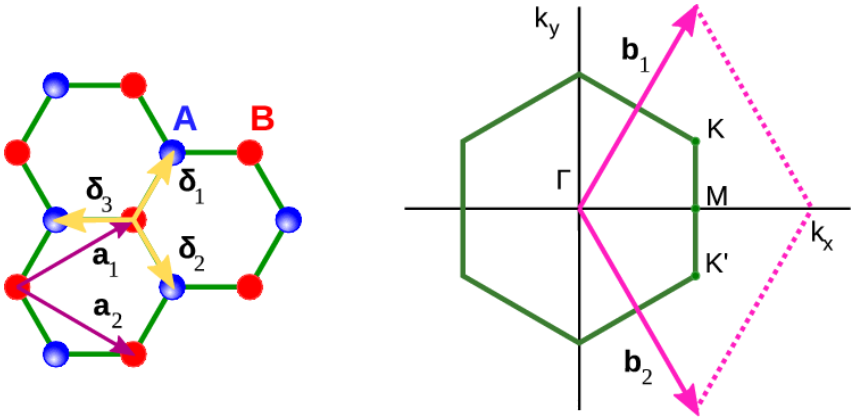

Fig. 4: Graphene lattice in real and reciprocal space. The vectors $\mathbf{a}_1$ and $\mathbf{a}_2$ are matched by the $\mathbf{b}_1$ and $\mathbf{b}_2$ vectors in the reciprocal space

Thanks to its unique properties, graphene became intensively investigated and is being used in many scientific and technological sectors. It is widely used in bio-sensing processes, mostly thanks to its electrochemical properties like high carrier mobility, the electrical sensitivity on adsorbing molecules, low thermal noise, biocompatibility etc. It can also be used for coatings, filtration, optoelectronic applications and many more.

4.1. Properties of graphene

In terms of mechanical properties, graphene evinces high tensile strength. In the experiment done by Lee and coworkers [15] pristine graphene was put under tensile load,

subsequently, its Young module was determined to be $E = 1$ TPa, that is one of the highest values among real materials.

Graphene has high thermal conductivity in order of 5000 W/mK [16], large surface area 2630 m^2/g [17] and is bendable, which is also used in several applications.[18]

In terms of electrical properties, among the most important and useful are a high carrier mobility at room temperature (theoretically 250 000 $cm^2V^{-1}s^{-1}$ [19], but only about 140 000 $cm^2V^{-1}s^{-1}$ [20] was measured) and a special band structure around the so called Dirac point, where the π bands exhibit linear dispersion (as shown in Fig. 5).[21]

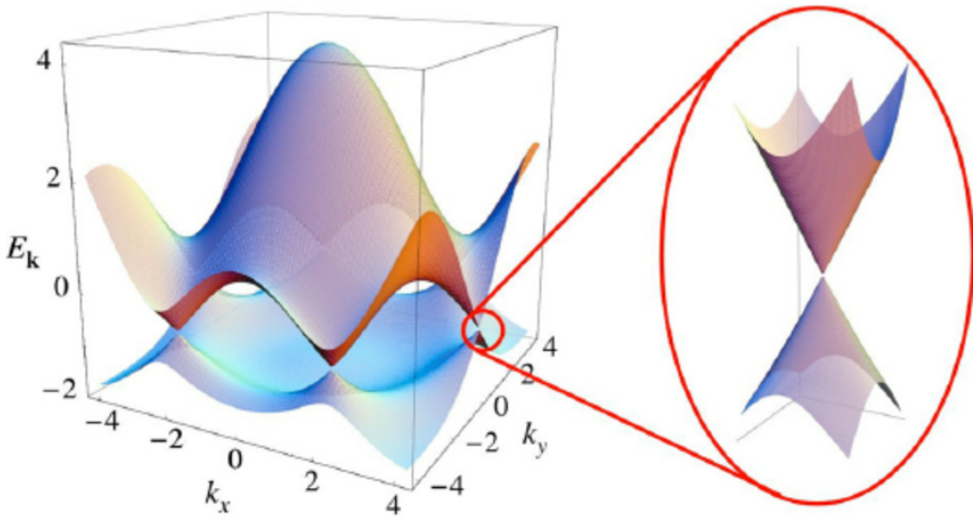

Fig. 5: Graphene band structure with linear dispersion around the Dirac point, adapted from [22].

The Fermi level in pristine graphene is theoretically right in the Dirac point, so there is no predominant type of charge carriers (electrons or holes). By applying a gate voltage in field effect transistor architecture to graphene, we can change the Fermi level and dope graphene with electrons or holes.

4.2. CVD graphene growth

There are several methods for graphene preparation. Firstly, there is a mechanical exfoliation that was used also by Geim and Novoselov when they made graphene for the first time. The next commonly used method is the reduction of graphene oxide. This thesis

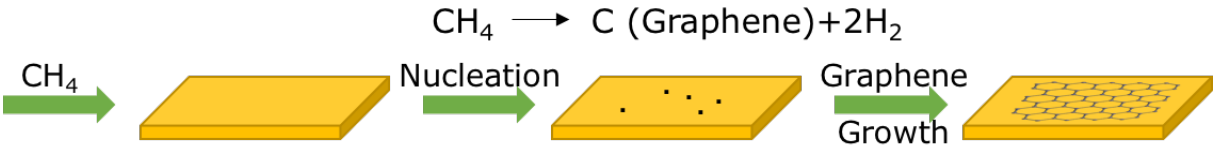

Fig. 6: The CVD process. The carbon gasses are pumped into the reaction chamber where they form a graphene monolayer on the surface of the metal substrate.Adapted from [24]

deals with a sensor that contains a graphene sheet made via chemical vapour deposition (CVD), so this method will be described in more details.

During the CVD process (Fig. 6), the carbon atoms form a graphene layer on a catalytic substrate. The metal substrate is put into the reaction chamber and subsequently, a mixture containing carbon gasses (e. g. methane) is drifted into the chamber where the substrate is heated. In the chamber, the carbon gasses are decomposed to individual atoms. Some atoms from the main stream start to move in the direction of the substrate and adsorb on its surface. Some of them are desorbed back to the main stream. On the substrate surface, a group of carbon atoms form a nucleation island and the others move to it thanks to diffusion. This is how a mono-layer graphene sheet is formed on the substrate. The remaining gasses are pumped out of the chamber and the substrate is cooled down to room temperature.[23][22]

5. Graphene field effect transistor (GFET)

A field effect transistor (FET) is a device, which has three electrodes. Two of them, drain and source, are conductively connected. On the conducting channel lies a layer of insulator, typically an oxide, on top of the insulator is the third, gate electrode. The oxide electrically separates the conducting channel from the gate. If we put some potential (voltage) V_g on the gate, charge will accumulate on the top side of the oxide. On the opposite side of the oxide in the conducting channel the opposite charge -Q will accumulate, making the system a capacitor. Its capacity is given by the relation.[25]

$$C = Q/V_g \tag{5.1}$$

If we consider the bottom-gated FET, the insulating layer is underneath the conducting channel. This makes it possible to place an electrode under this insulator thus creating a bottom gate electrode (Fig. 8). The gates are not always solid materials but can be also in liquid phase.

In dual gated graphene field effect transistors (GFET), the conducting channel is formed by a layer of graphene. Due to the graphene's 2 dimensional nature and surface density of charge carriers the concentration of charge carriers, $n_{e,h}$ can be derived from equation (1) and depends linearly on the gate voltage V_g, by formula [25]

$$n_{e,h} = \alpha \cdot V_g \tag{5.2}$$

where α is a charge injection rate:

$$\alpha = \frac{\epsilon_0 \epsilon_r}{ed} \tag{5.3}$$

Where ϵ_0 is the permitivity of vacuum, ϵ_r is relative permittivity of the material, e is the elementary charge and d is thickness of the layer.

Graphene exhibits the lowest conductivity and so the highest resistivity and resistance when the Fermi level is in the Dirac point having no prevalent type of charge carriers and

strongly reduced number of states when the Fermi level is in the Dirac point. By applying different gate voltages V_g we can change the Fermi level in graphene. This causes one type of the charge carriers to become prevalent and the capacity of the capacitor to change.

5.1. Liquid top-gate GFET

As established in the previous paragraphs, the insulating layer in the top gate can be either solid or liquid. The solid insulation behaves as described at the beginning of this chapter. In the case of a liquid phase top gate a droplet of highly resistive solution is used to separate the top gate electrode from the channel(Fig. 7). By putting potential on the top gate electrode, some ions from the solution get immobilized on the graphene surface forming a layer. Then, other ions from the solution with opposite charge form another layer on top of the first layer. This arrangement is called an electrolytic double layer and its thickness is a very important quantity called Debye length λ_D. It is given by following formula [26]:

$$\lambda_D = \sqrt{\frac{\epsilon k_B T}{2 N_A e^2 I}} \tag{5.4}$$

Where k_B is Boltzman constant, N_A is Avogadro constant, ϵ is the the permittivity of the material, T is absolute temperature, e is the elementary charge and I is ionic strength of the solution.

The Debye length describes the maximal distance from the surface in which the ions from the solution are able to interact with the graphene channel and so influence its properties.

5.2. Dual-gate GFET

In the experimental part of this work the dual-gated GFET was used, meaning that it have both a top-gate and a bottom-gate and different voltages can be applied to each of the gates individually. Having both gates and also being able to apply different voltages to each of them makes it possible to measure both the marginal influences of both gates as well as the collective influence both gates have on the response of the sensor.

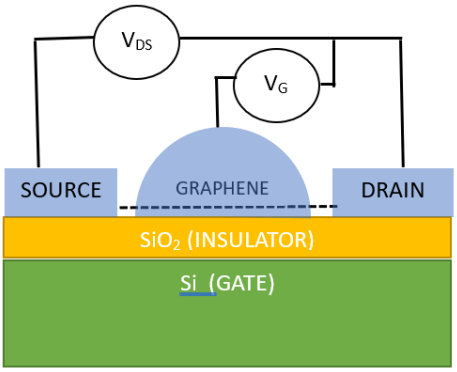

Fig. 7: The sensor in top gate configuration with liquid top gate

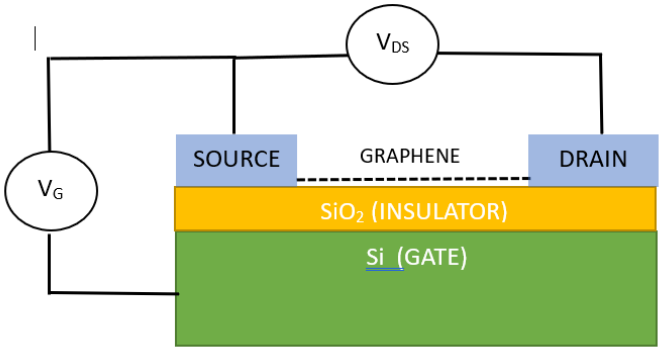

Fig. 8: The sensor in bottom gate configuration

6. Search

In the search part I focused on 2 topics. The first one is glucose sensing using GFETs and the second is applications of dual gated GFETs.

6.1. Gucose sensing using GFETs

In 2020 Huang C. et al. prepared GFET for sensitive glucose sensing. Graphene was functionalized with Pyrene - 1 - Boronic acid. Its limit of detection (LOD) was established to 0.15 µM with detection range from 0.05 to 100 mM. The useful and uncommon innovative property of this sensor was its bendability, which is useful in medicine applications.[27]

In 2022 Fenoy G. E. et al. prepared GFET sensor for urine glucose detection. The graphene layer lies on golden raster and is functionalized with poly(3-aminobenzyl-co-aniline) and Glucose oxidase. This sensor shows LOD 4.1 µM and detection range from 10 to 1000 µM. [28]

6.2. Dual gated GFETs

Dual gated sensor with honey as dielectric

In 2021 Alzaid M. et al. prepared dual gated graphene field effect transistor and performed it with honey as a top gate dielectric. Graphene was grown by CVD on Cu foil, then covered by PMMA. Afterwards the Cu was etched, and the graphene was shifted on p-Si substrate with 300 nm SiO_2 layer. Then the metal contacts were deposited by thermal evaporator.

During the measurement the honey in 2 mm thick layer was swept from one side of the channel to another. The measurement was made in 3 different states. First measurement with back gate was taken with pristine graphene and the Dirac point was found at -2 V. During the second measurement with channel half covered with honey, 2 local current minima were found at – 35 V and 0 V. The last measurement with channel fully covered with honey, the Dirac point shifted to – 32 V.

The second part of the experiment measured the dependency of current in the channel on the back gate voltage for top gate voltages from 3 V to -4 V, with step of 1 V. The

gradual shift of Dirac point (current minima) voltage was observed increasing from about -50 V to nearly 0 V with increasing top gate voltage. [29]

Dual gated Graphene FET pressure sensor with movable top gate

In 2020 Tamersit K., Kotti M. and Fakhfakh M. constructed dual gated GFET pressure sensor with movable top gate. Its top gate was not fastened to the top of the insulating oxide, but it was able to move in the vertical direction depending on the applied pressure. The distance between the movable top gate and the oxide influences the capacity on the top gate and so the current in the conducting channel.

When applied back gate voltage V_{BG} = -40 V and the voltage V_{DS} = 0.5 V on the channel electrodes, we can observe the linear shift of the Dirac top gate voltage from about 11.5 V to 3 V when changing the distance of the top gate electrode from 15 nm to 0 nm.[11]

Dual gated GFET with improved radio frequency

In 2009 Lin Y-M. et al. constructed GFET and tested the optimal applied voltages to reach the highest possible frequency. They realized that the best radio frequency is reached when the conductance of the channel is minimal. They realized that the lowest conductance is reached when top gate V_T = 1.5 V and back gate V_B = -40 V is applied.

In very similar configuration with V_T = 1.6 V, V_B = -40 V and the channel voltage V_{CH} = 0,8 V they tested how the frequency depend on the current gain. The measurement shown that the cut-off frequency of the sensor is 50 GHz. [30]

7. Experiment

7.1. Droplet evaporation

When measuring with a top-gate configuration, a droplet of the measured liquid acts as a dielectric layer. Its typical volume is in the order of tens of µl. The droplet evaporates over time, which can influence the measurement. Therefore, in order to determine whether it is necessary to account for this evaporation during regular measurements, a documentation of the deionized (DI) water droplet evaporation was studied as shown in Fig. 9 and Tab. 1.

During the measurement, the liquid droplet is put on a silicon wafer with a graphene layer. 1 µl droplet is put on the surface of a silicon wafer and imaged by optical microscope every 30 s. After the photographs were processed, the decreasing radius of the droplet was measured. Based on fact that the droplet kept a hemisphere shape most of the time, its expected volume and surface can be calculated for every time frame (Tab.7.1.).

Tab.7.1.: The measured radii and calculated volume and surface of the evaporating droplet.

time (s)	0	30	60	90	120	150	180	210	240	270
radius (px)	727.0	690.0	648.5	607.0	565.5	513.0	472.5	410.5	350.0	279.5
volume (µl)	1.000	0.860	0.714	0.585	0.473	0.353	0.276	0.181	0.112	0.057
surface (mm^2)	8.30	7.47	6.60	5.78	5.02	4.13	3.50	2.64	1.92	1.22

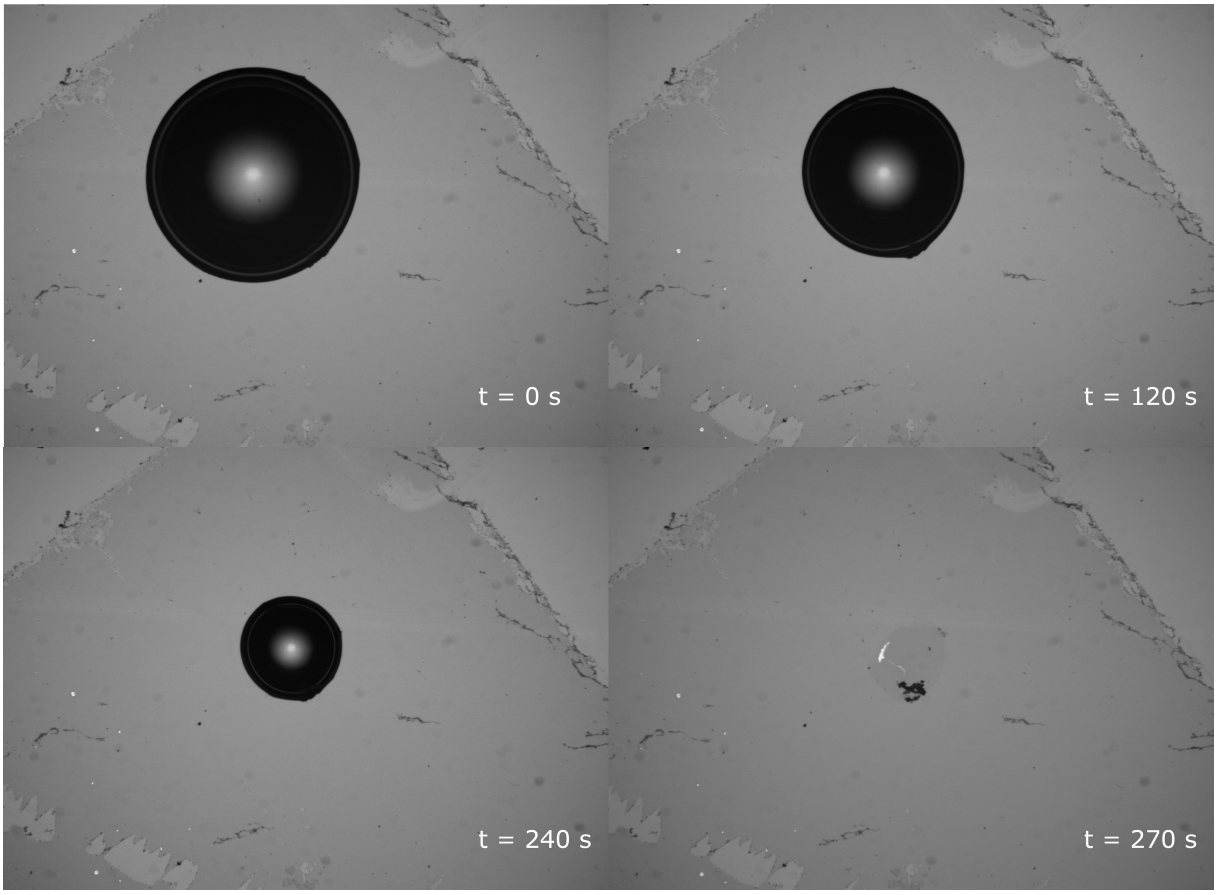

Fig. 9: The optical microscopy pictures showing the water droplet evaporation right after it was put on the graphene surface in time. The droplet evaporated completely between 240 and 270 s. In the last picture there is no remaining water on the graphene surface, the round object in the middle of the picture is damaged graphene and water impurity residuals.

7.2. Functionalization process

The sample, a SiO_2/Si wafer with golden electrodes and graphene mono-layer, is first immersed in the 5 mM solution of PSE in DMF for 2 hours at room temperature. This solution was prepared by dissolving of 10 mg of PSE in 5 ml of DMF. After that the sample is washed by Isopropylalcohol (IPA) and DI water.

After that the sample is taped on a slide with one wire stuck down on the bottom of the sample (between the sample and the slide) with silver paste. This wire serves for application of bottom gate voltage. After that the ends of the golden electrodes that leads from the drain and source electrode of the capacitor are also conductively connected with

the wires with silver paste. In the end the wires are taped to the slide in order not to break of the silver paste connection.

The last step is to put a 50 µl droplet of glucose oxidase solution on the graphene surface. The solution is prepared by dissolving of 10 mg of glucose oxidase in 1 ml of 1xPBS. The sensor thus prepared is now put in to the fridge for 10 to 16 hours. After this time spent in the fridge the glucose oxidase solution is rinsed with 1xPBS and DI water.

7.3. Sensor measurement

The measurement is performed on the electronic measuring station. The lock-in amplifier Stanford research SR 830 was used for measuring electrical characteristics and was connected to 10 MΩ resistor. The gate voltage was supplied by a Keithly 6221 AC/DC current source connected to 1 MΩ parallel. The time constant was 100 ms and the frequency 1333 Hz.

Bottom gate configuration

When measuring with a bottom-gate configuration the 30 µl liquid droplet is put on the graphene surface, subsequently, the bottom-gate voltage is swept from 0 V to 80 V then down to -80 V and then back to 0 V again by steps of 1 V/1 s. The measurement output describes the dependency of channel resistivity to bottom gate voltage. In the first measurement a solution of 0.01 mM PBS was measured, followed by 25, 50 and 100 mM glucose solutions. All glucose solutions used during whole experimental part were prepared by dissolving glucose in 0.01 mM PBS.

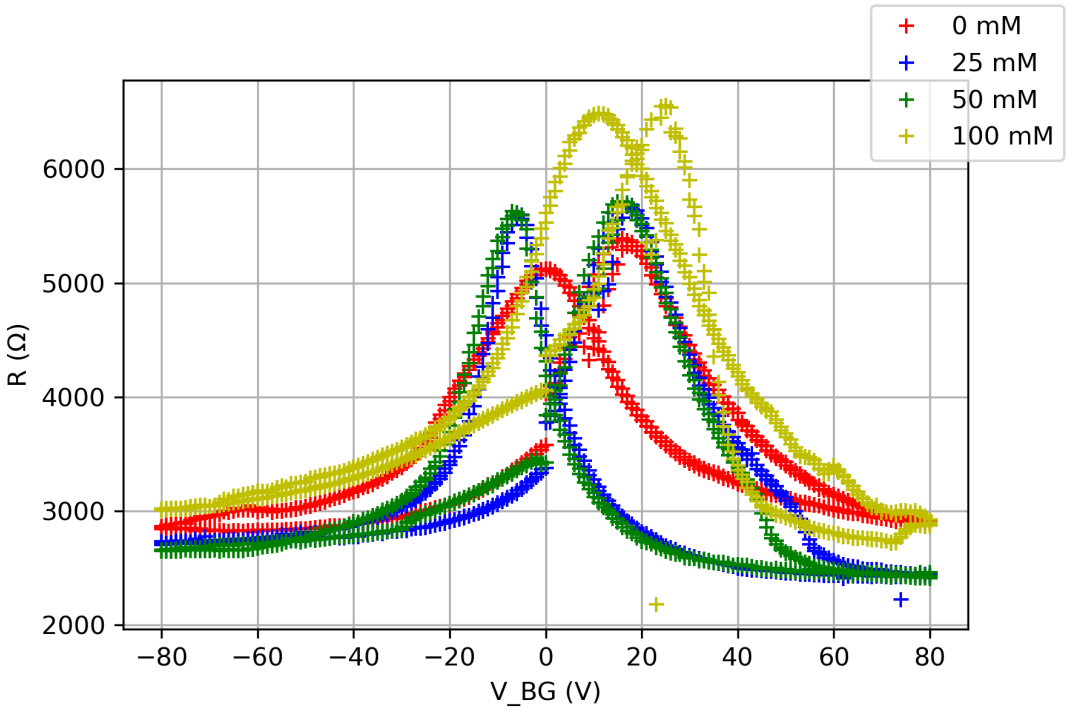

Fig. 10: The bottom gate measurement of Dirac point voltages for concentrations of 0 mM, 25 mM, 50 mM and 100 mM.

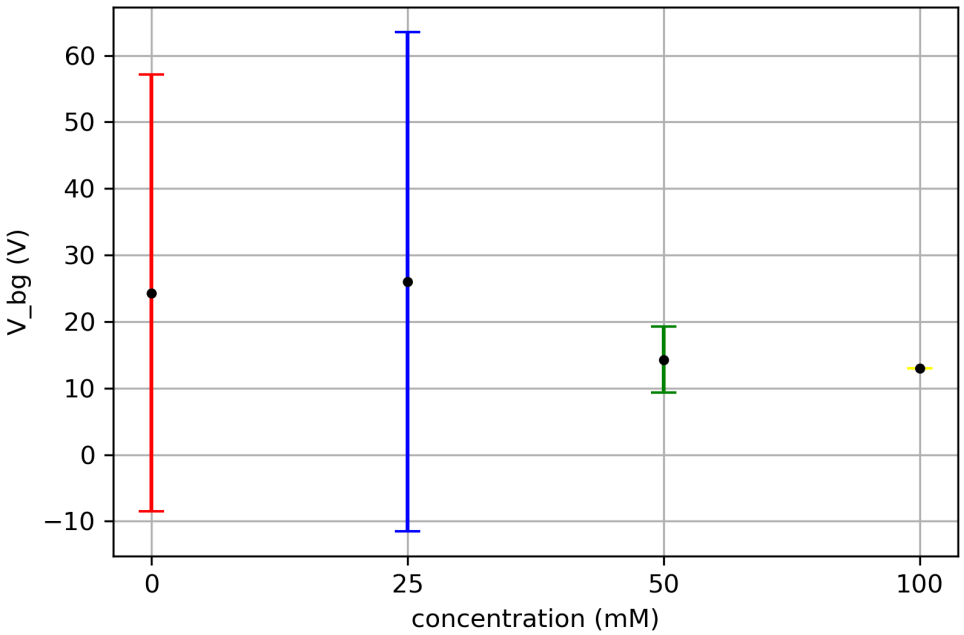

Fig. 11: The uncertainties intervals of the Dirac point voltages for the 4 measured concentrations in bottom gate configuration.

In the Fig. 10 there is resistivity vs. back gate voltage for four different concentrations. The theory says that the value of the Dirac point voltage grows with the concentration of the solution. The graph shows that for the highest concentration the Dirac point voltage is strongly higher than for other concentrations. The concentrations of 0 mM, 25 mM and 50 mM, the Dirac point voltage differs only a little.

Fig. 11 shows the uncertainties intervals of the Dirac point voltages in the back gate configuration. Each concentration was measured 3 times and the Voltages were subsequently statistically processed. The plot shows that the higher concentrations gives more stable results.

Top-gate configuration

In the top gate configuration 10 µl droplet of the measured solution is pipetted on the graphene surface, now the top gate voltage is swept from 0 V to 1.5 V then to -1.5 V and back to 0 V. The step is 0.01 V each 0.5 s. The same solutions were measured as in the bottom gate configuration, so the 0.01 mM PBS and 25, 50 and 100 mM glucose solutions.

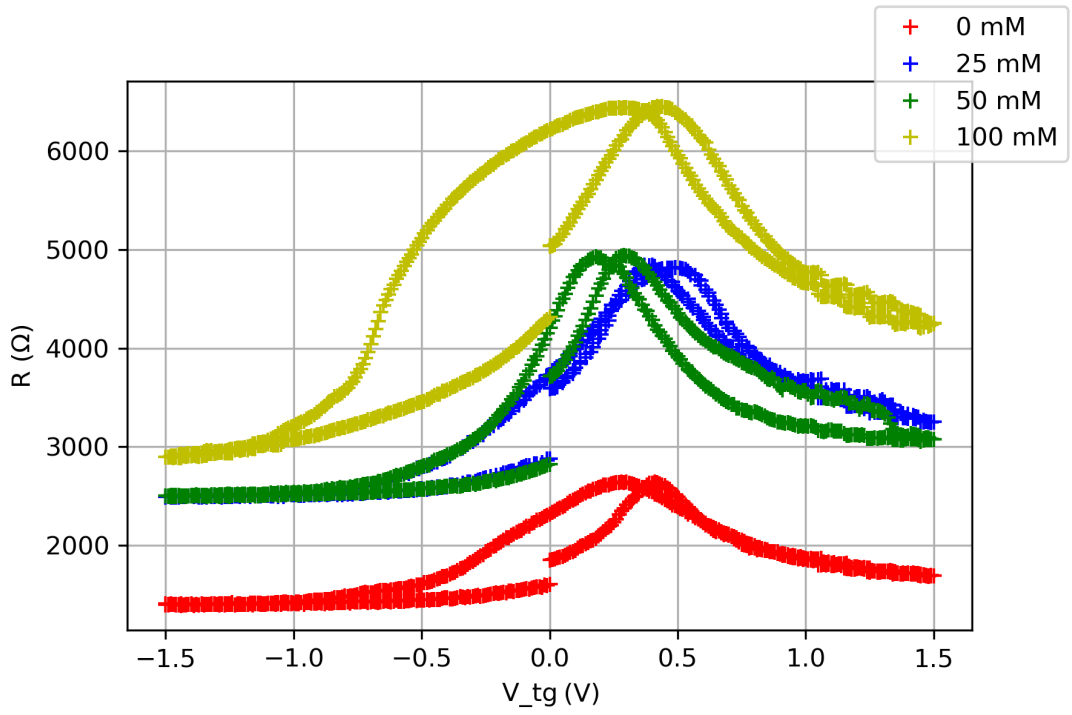

Fig. 12: The top gate measurement of Dirac point of glucose concentrations 0 mM, 25 mM, 50 mM and 100 mM.

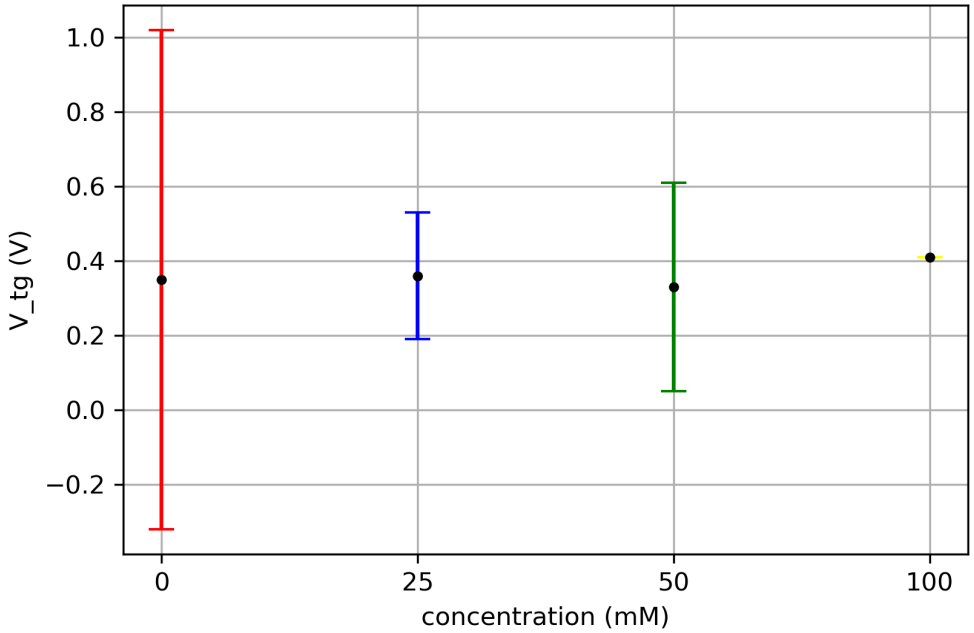

Fig. 13: The uncertainties intervals of the Dirac point voltages for the 4 measured concentrations in the top gate configuration.

In case of the bottom gate measurement (Fig. 12) there is no significant change in the Dirac point voltage for growing concentration. The uncertainties intervals for the Dirac point voltages again show that the results are more stable for higher glucose concentrations.

Time series

The next measurement tests how the sensor reacts on the different glucose concentrations when applied a constant voltage. For the first measurement of time series, zero gate voltage is applied, we know that Dirac points voltages of all measured solutions lies above this value, so we measure in p doping. The measurement starts with sample without any solution droplet. After about 1 min first droplet of glucose solution of 5 mM concentration and 10 µl volume is put on the sample. After about 100 s the first droplet is replaced with the next one of a solution of the different glucose concentration. The whole procedure is repeated for another concentrations during the experiment. The tested concentrations (in mM of glucose) were measured in the following order : 10, 12, 14, 23, 32, 14, 12, 8, 5. Finally, a droplet of DI water is measured. The results are presented in Fig. 14:

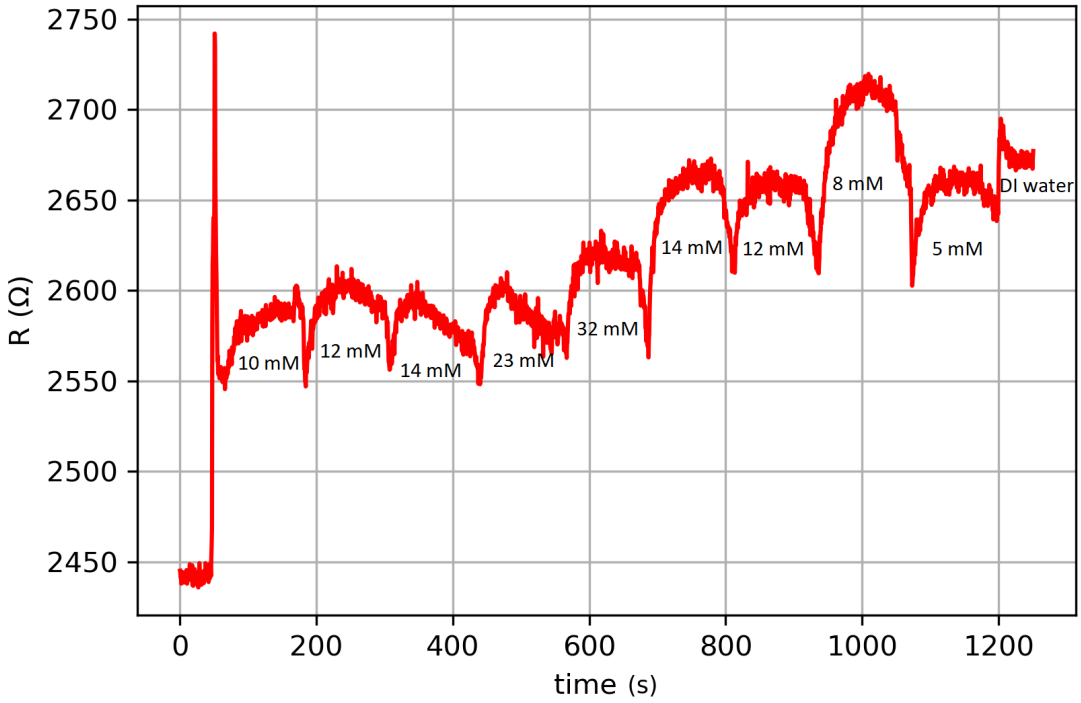

Fig. 14: Time series with $V_g = 0$ V. The concentrations were swept approximately every 100 s.

As can be seen in Fig. 14 the different concentrations change the resistivity of the sensor only slightly when changed with that time step. But the interesting phenomena is the jump in resistance after the highest concentration is measured and the next droplet of lower concentration is added.

After the first time series the second one is done with different concentration series and different time step (Fig. 15). The gate voltage is set to 0 V as in previous measurement. The concentrations were tested in the following order (in mM): 5, 10, 16, 21, 25, 32, 21, 10. Now the time for which each droplet is measured is about 4 minutes for the first 6 droplets(5 mM to 32 mM), when the concentration increased. The last 2 droplets (21 mM, 10 mM) were measured for about 8 minutes each because it took longer time to stabilize the sensor resistivity. The following plot shows the results.

It can be seen, that the longer time step between sweeping of concentrations enables the resistivity to stabilize and gives more awaited results. The resistivity grows even when the concentration decreases which happened also in the previous measurement. That can be caused by continuous degradation of the sensor during the measurement, that causes

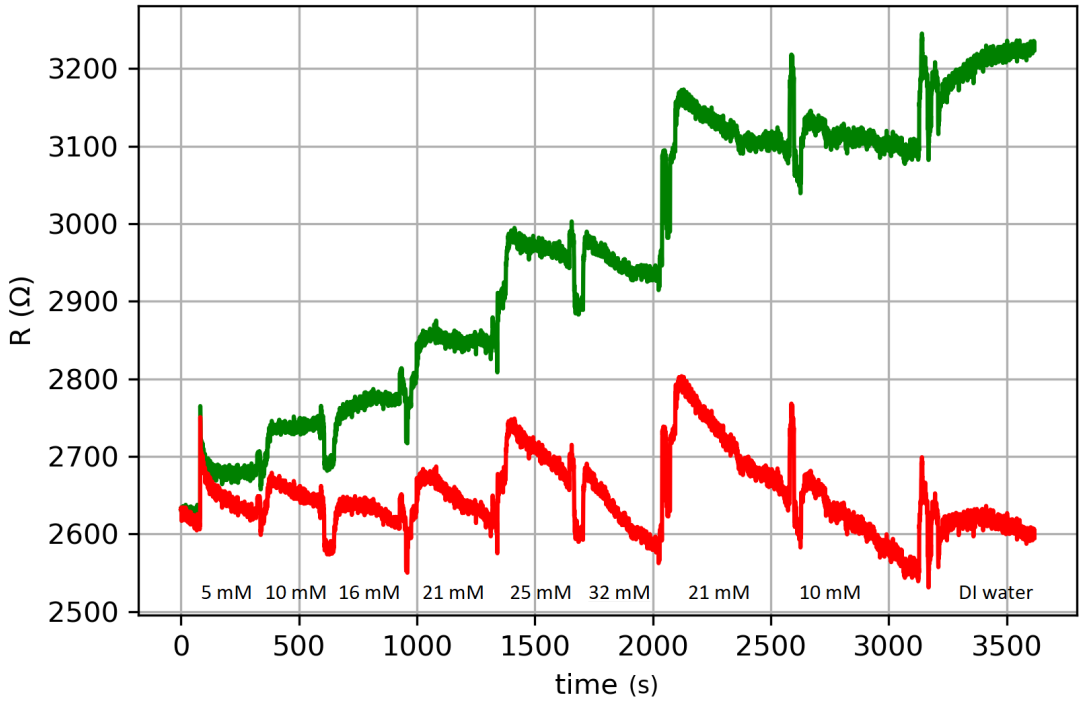

Fig. 15: The green line shows the real results in time series with $V_g = 0$ V. The concentrations were swept approximately every 4 minutes, the last two droplets were left on the sensor for 8 minutes. The red line shows the results when linear increase from minimal to maximal volume is subtracted.

continuous increase in resistivity as is also visible when comparing the resistivity measured for the same concentrations in Fig. 14 and Fig. 15.

Both measurements above are done also in the top gate configuration with top gate voltage 1 V (Fig. 16, 18), and for bottom gate measurement with bottom gate voltage 50 V (Fig. 17, 18) all on one sensor. Both voltages are above the Dirac point voltages of all measured concentrations in given configuration. It means that graphene was n-doped. The following plots show the results:

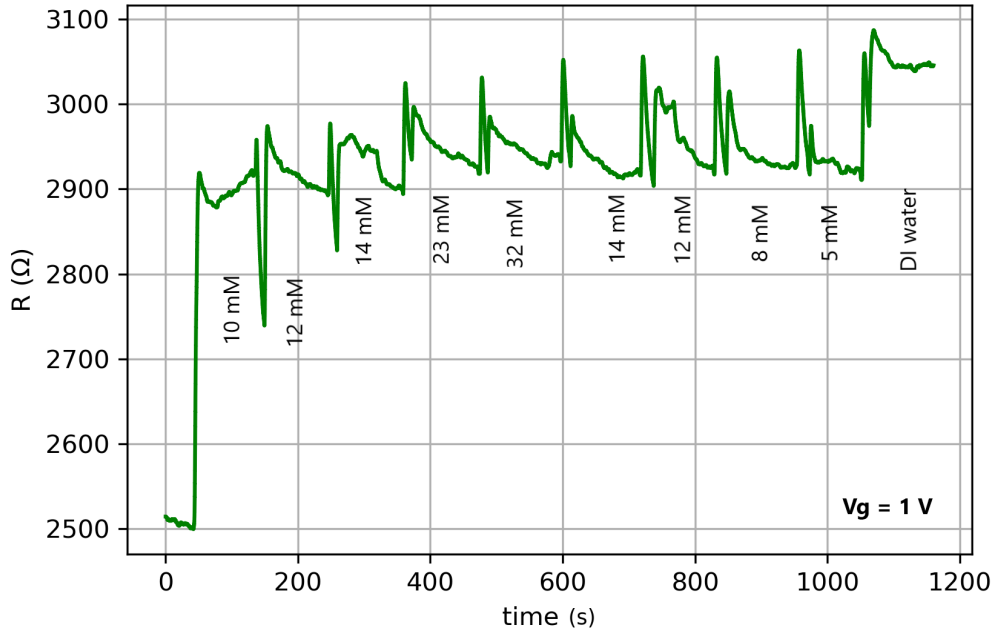

Fig. 16: Time series with top gate voltage $V_g = 1$ V. The concentrations were swept approximately every 100 s.

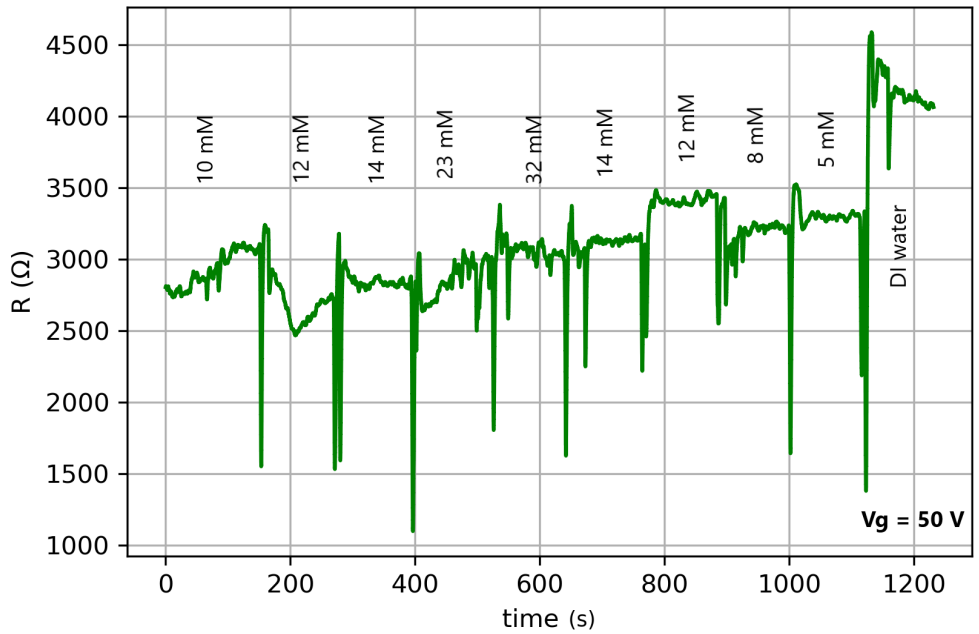

Fig. 17: Time series with bottom gate voltage $V_g = 50$ V. The concentrations were swept approximately every 100 s.

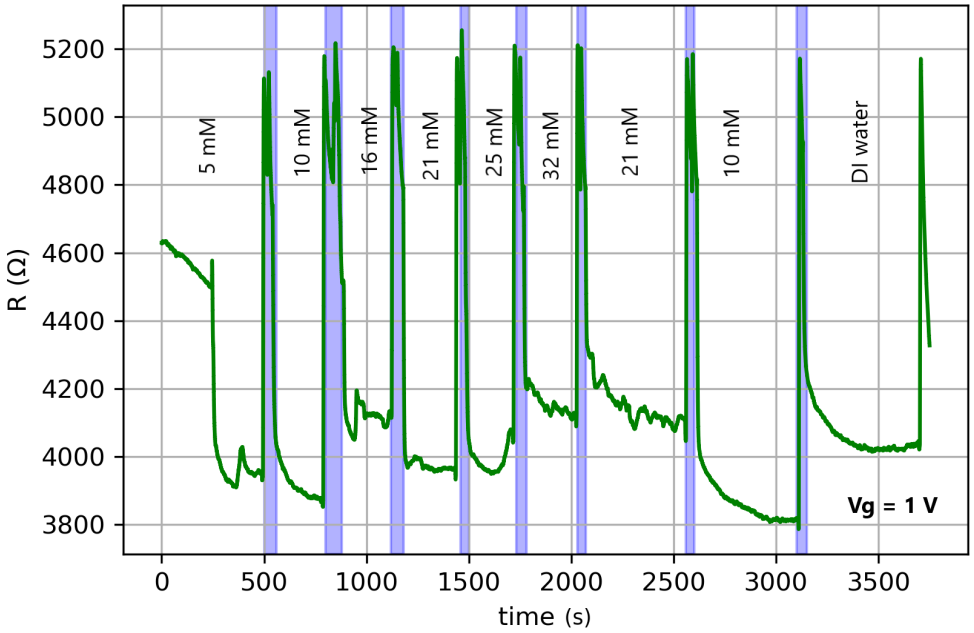

Fig. 18: Time series with top gate voltage $V_g = 1$ V. The concentrations were swept approximately every 4 minutes.

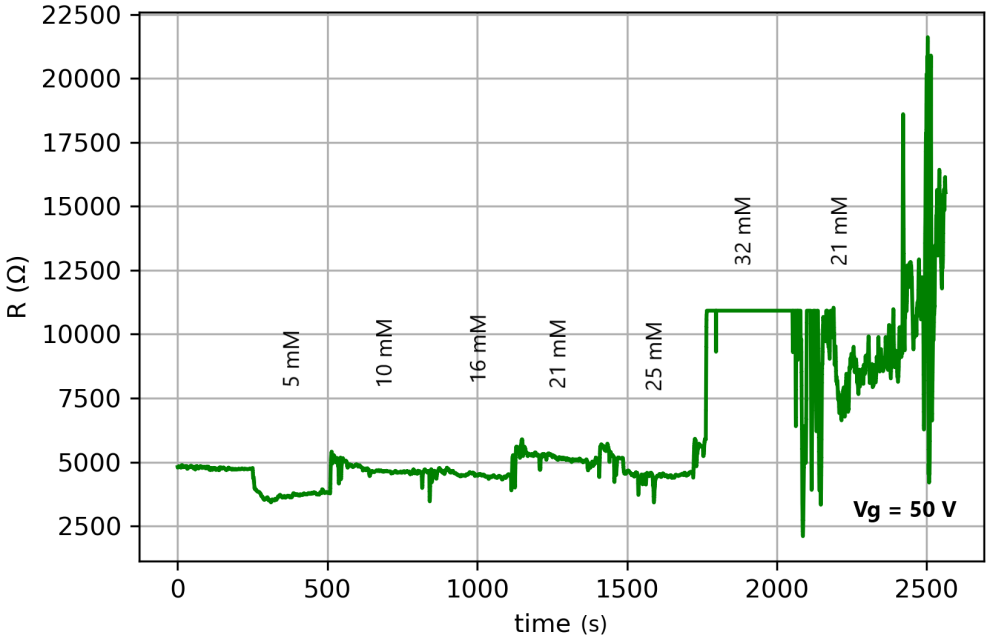

Fig. 19: Time series with top gate voltage $V_g = 50$ V. The concentrations were swept approximately every 4 minutes.

Fig. 16 shows that the sensor reacted awaited way only for the first 4 concentrations, after that the response started to be similar for every tested concentration. It also shows that 100 s is not enough time for the sensor to stabilize the reaction. The next measurement which results are shown in Fig. 17 was done with bottom gate voltage 50 V and the results show that the bottom gate configuration tends to stabilize in shorter time, so that 100 s is sufficeient. On the opposite hand the response of the sensor doesn't show any regular dependency on glucose concentration of measured solution.

The last two figures (Fig. 18 and Fig. 19) shows the results when the droplet was left on the sensor for longer time (4 minutes). The results show similar phenomenon as the ones of the previous measurement, thus in the top gate configuration 4 minutes are still not enough time for the sensor to stabilize, while in the bottom gate configuration the stabilization time is shorter. The blue columns in Fig. 18 shows the periods of time when the sensor was rinsed with DI water. That was done in expectation that the water can wash the glucose from the surface of the electrodes and the sensor would react more precisely on the given concentration. The results point out that this additive step doesn't give better results.

During the last measurement (Fig. 19) the sensor raised its resistivity in a leap when 32 mM solution was tested. That has to be considered as some technical issue or breaking gate so there was no point in continuing the experiment. The flat line of resistivity when 32 mM solution was tested is not the real measured resistivity, but it is the maximal allowed value because of the adjusted limit of the sensitivity.

All 4 measurements of time series were measured on one sample and the same phenomena as in Fig. 14 and 15 can be seen. The resistivity grows during the measurement because of the sensor degradation.

8. Conclusion

In this thesis double gated graphene field effect transistor was studied and its response was tested for glucose solutions in wide range of concentrations (from 5 mM to 100 mM). The aims of this thesis are to investigate the response of the sensor in the top gate and the bottom gate configuration.

The measurement was done via selective approach, so the graphene surface was functionalized before measurement. The functionalization was done by bonding of PSE as linker molecule and Glucose oxidase as biorecognition element.

The first measurement determined the Dirac point voltages for glucose solutions of concentrations of 25 mM, 50 mM and 100 mM in the top gate and in the bottom gate configuration. It has been realized, that the higher the glucose concentration is, the higher the Dirac point voltage is, which means the graphene is more p-doped and the glucose acts as electron acceptor.

The next measurement studied how the sensor react when the concentration of measured solution changes in time. The concentration series increased for the first half of measurement and subsequently decreased. There are two general findings. The first one is that the resistance stabilize in shorter time in the bottom gate configuration. The second one is that the resistivity tends to rise in a leap when the concentration starts to decrease.

In the previous 2 years similar experiments were done here on the IPE and presented in Bachelor thesis. The results in time series shows more linear dependency on concentration and shorter stabilization time of the resistance in comparison with the results presented in this thesis. In the Dirac point voltage measurement, lower concentrations of glucose were measured and what is most important negative values of the Dirac point voltages were found which is in oppose to the results presented in this thesis. For the back gate voltage and concentration of 32 mM The shift in Dirac point voltage was about 1 V relative to 0.01 M PBS solution. During my measurements the shift was also small for concentrations around this value (about 2 voltes for concentrations of 25 mM and 50 mM), but it reached 13 V for 100 mM solution.

Bibliography

[1] MALHOTRA, S., et al.: Biosensors: Principle, types and applications . *IJARIIE*, Vol-3 Issue-2 2017, p. 3639 - 3644. ISSN 2395-4396.

[2] SAID, N. A. M., OGURTSOV, V. I. and HERYOG, G.: Electrochemical biosensor based on microfabricated electrode arrays for life sciences applications. *Biomaterials Research*, 2014, doi: 10.13140/RG.2.2.11066.49603.

[3] HARDEEP, K., AAKASH, B. and SURAJ, S.: Biosensors: Classification, Fundamental Characterization and New Trends: A Review . *International Journal of Health Sciences Research*, 315, Vol.8; Issue: 6; 2018, P. 315 - 333, ISSN: 2249-9571.

[4] HAITAO LI, et al.: CMOS Electrochemical Instrumentation for Biosensor Microsystems: A Review. *Nanobiosensing for Sensors* , 2017, 17(1) doi: 10.3390/s17010074.

[5] DAMBORSKY, P., KATRLIK, J. and SVITEL, J.: Optical biosensors. . *Essays in Biochemistry*, 2016; 60(1): p. 91–100, doi: 10.1042/EBC20150010.

[6] SIEGEL, T. W., et al.: Purification and properties of the human placental insulin receptor. . *Journal of Biological Chemistry*, 1981. p. 9266 - 9273; vol. 256, No 17.

[7] POHANKA, M.: *Přehled biochemie*. Fakulta vojenského zdravotnictví, Univerzita obrany. 2017. ISBN: 978-80-7231-358-7.

[8] NIH: Blood Glucose. *MedlinePlus*, NIH: National Institute of Diabetes and Digestive and Kidney Diseases. https://medlineplus.gov/bloodglucose.html.

[9] MOOR, D.: David Moore's World of Fungi: Fungiflex - the untold story . *https://davidmoore.org.uk/fungiflexweb/F-flex*$_1$*0.htm*.

[10] IL-HOON, Ch., DONG, H. K. and SANGSOO, P.: Electrochemical biosensors: perspective on functional nanomaterials for on-site analysis. *Biomaterials Research* , 2020; 24, doi: 10.1186/s40824-019-0181-y.

[11] PAPAGEORGIOU, D. G., KINLOCH, I. A. and YOUNG, R. J.: Mechanical properties of graphene and graphene-based nanocomposites. Progress in Materials Science, Volume 90, 2017, p. 75-127. DOI: 2017.07.004.

[12] *MERCK* [Online] [accessed: 12.4.2023] Available at https://www.sigmaaldrich.com/CZ/en/product/sial/227056

[13] *MERCK* [Online] [accessed: 12.4.2023] Available at https://www.sigmaaldrich.com/CZ/en/product/sial/457078

[14] FOA TORES, L. E. F., ROCHE, S and CHARLIER, J-Ch.: *Introduction to Graphene-Based Nanomaterials*. Cambridge University Press, 2020. ISBN 9781108664462. DOI: 10.1017/9781108664462

[15] LEE, Ch., et al.: Measurement of the elastic properties and intrinsic strength of monolayer graphene. Science, 2008, 18;321(5887):385-8. doi: 10.1126/science.1157996.

[16] BALANDIN, A. A., et al.: Superior thermal conductivity of single-layer graphene. Nano Lett, 8 (3) (2008), p. 902-907. DOI: 10.1021/nl0731872.

[17] ZHU, Y., et al.: Graphene and graphene oxide: synthesis, properties, and applications. Adv. Mater., 2010, 22 (35), p. 3906-3924. DOI: 10.1002/adma.20100106

[18] OVIDKO, I. A.: Enhanced mechanical properties of polymer-matrix nanocomposites reinforced bygraphene inclusions: a review. Rev. Adv. Mater. Sci., 2013(34); p. 19-25.

[19] NOVOSELOV, K., et al.: Two-dimensional gas of massless Dirac fermions in graphene. Nature, 2005, 438 (7065) , p. 197-200. DOI: 10.1038/nature04233.

[20] TSUNEIA A.: Zero-mode anomalies of massless Dirac electron in graphene. *Jour. of Appl. Phys.* 2011 Vol. 109, Issue: 10, DOI: 10.1063/1.3575639

[21] McClure, J., V.: Band Structurure of Graphite and de Haas-van Alphen Effect *Appl. Sci.* 1957, Vol. 108, Num. 3., p. 612 - 618

[22] MAFFUCCI, A. and MIANO, G.: Electrical Properties of Graphene for Interconnect Applications. *Appl. Sci.*, 2014; ISSN 2076-3417, DOI: 10.3390/app4020305.

[23] *GRAPHENEA* [Online] [accessed: 28.3.2023] Available at: https://www.graphenea.com/pages/cvd-graphene.ZCrN3nZByUk.

[24] CVD Graphene [Online] [accessed: 29.3.2023] Available at: https://www.acsmaterial.com/blog-detail/cvd-graphene.html.

[25] HALLIDAY, David, Robert RESNICK a Jearl WALKER, DUB, Petr, ed. Fyzika. 2., přeprac. vyd. Brno: VUTIUM, c2013. Překlady vysokoškolských učebnic. ISBN 978-80-214-4123-1.

[26] MALATINOVÁ, M. Double-gate biosensor of glucose based on functionalized graphene. Brno: Vysoké učení technické v Brně, Fakulta strojního inženýrství, 2022.

[27] HUANG, C., et al.: An integrated flexible and reusable graphene field effect transistor nanosensor for monitoring glucose. Journal of Materiomics, Vol. 6, Issue 2, 2020, p. 308-314. DOI: 10.1016/j.jmat.2020.02.002

[28] FENOY, G. E., et al.: Highly sensitive urine glucose detection with graphene field-effect transistors functionalized with electropolymerized nanofilms. Sensors Diagnostics, 2022, 1, p. 139–148. DOI: 10.1039/ d1sd00007a.

[29] ALZAID M., et al.: Charge carrier modulation in dual-gated graphene field effect transistor using honey as polar organic gate dielectric. *Applied Phyyics A*, 2021, vol. 127, p. 1-7. DOI = 10.1007/s00339-021-04581-y

[30] LIN Y-M., et al.: Dual-Gate Graphene FETs With fT of 50 GHz. IEEE, 2009, vol. 31 (1), p. 68 - 70. DOI: 10.1109/LED.2009.2034876.

List of abreviations

DMF	NN-dimethylformamide
PSE	1-Pyrenebutiric acid N-hydroxysuccinimide ester
PBS	Phosphate buffer saline
CVD	chemical vapour deposition
FET	field effect transistor
GFET	graphene field effect transistor
PMMA	polymethyle metacrilate
DI water	deionized water